https://doi.org/10.20965/jaciii.2019.p0823

Paper:

Asymmetric MF-DCCA Method Based on Fluctuation Conduction and its Application in Air Pollution in Hangzhou

Chaohui Xiang, Xiaozhen Hao, Wenhui Wang, and Zhenlong Chen†

School of Statistics and Mathematics, Zhejiang Gongshang University
No. 18, Xuezheng Street, Xiasha University Town, Hangzhou 310018, China
E-mail: zlchen@zjsu.edu.cn
†Corresponding author

[Received October 24, 2018; accepted January 11, 2019]

The study of the relationship between the concentration of $PM_{2.5}$ and the local air quality index (AQI) is significant for the improvement of urban air quality. This study not only considered multifractal cross-correlation but also the fluctuation conduction mechanism. An asymmetric multifractal detrended cross-correlation analysis (MF-DCCA) method based on fluctuation conduction is introduced here to empirically explore the causality and conduction time between air quality factors and $PM_{2.5}$ concentration. The empirical results indicate the existence of a bidirectional fluctuation conduction effect between $PM_{2.5}$ and PM_{10}, SO_2, and NO_2 in Hangzhou, China, with a conduction time of 30 hours; this effect is non-existent between $PM_{2.5}$ and O_3. In addition, there is a unidirectional fractal fluctuation conduction between $PM_{2.5}$ and CO with a conduction time of 21 hours.

Keywords: symmetric MF-DCCA, fluctuation conduction, causality, $PM_{2.5}$

1. Introduction

Atmospheric pollution has become a serious problem as a result of the current rapid economic growth and gradual expansion of the city of Hangzhou, China. Prior pollution events and their effects, such as the first recognized occurrences of photochemical smog in the United States in 1943, the Great Smog of London event of 1952, the recognition of asthma in relation to air pollutants in Japan in 1961, and the Bhopal incident in India in 1984, alert people to the necessity of air pollution control. Elevated concentrations of pollutants in the atmosphere can not only seriously harm human health, but also threaten the earth's ecosystems.

One of many air pollution factors currently in focus, the pollutant $PM_{2.5}$ is also referred to as fine particulates, whose diameter in the atmosphere is less than or equal to 2.5 μm. In October 2011, serious and persistent smog occurred in many areas such as China's Huang-Huai-Hai and the Yangtze River Delta. In the same year, the US Embassy in China detected local concentrations of $PM_{2.5}$ exceeding the relevant standard. These events were the catalyst that made $PM_{2.5}$ a topic of great concern to the public. As a result, China announced the "Environmental Air Quality Standards" (GB3095-2012) in the first half of 2012 to replace the original API (Air Pollution Index) with the current AQI (Air Quality Index). The current AQI now includes the particulate pollutant $PM_{2.5}$. This newly issued AQI is a dimensionless index composed of the indices of six pollutants, including inhalable particulates, referred to as PM_{10}, as well as particulates that can directly access the lungs, $PM_{2.5}$. Other pollutants included in the AQI are NO_2 (Nitrogen dioxide), SO_2 (Sulfur dioxide), CO (Carbon monoxide), and O_3 (Ozone). $PM_{2.5}$ is of obvious concern as it can enter the lungs directly and is a major cause of smog formation.

At present, the multifractal detrended cross-correlation analysis (MF-DCCA) method is widely used in the study of fractal characteristics of atmospheric environmental data. Vassoler and Zebende [1] used the DCCA method to analyze the fractal characteristics of the cross-correlation between relative humidity and average daily temperature in 50 regions of the world during the time period from 1997 to 2010; it was found that the degree of cross-correlation varies in different regions, which is mainly affected by seasonal factors. Kang et al. [2] analyzed the cross-correlation by the DCCA method between the hourly PM_{10} time series and three meteorological elements (temperature, wind speed, and relative humidity) in eight cities in Korea from January 2006 to December 2010, and found that the strength of cross-correlation between the various meteorological elements and PM_{10} is affected by the geographical location of the city. Hajian and Movahed [3] used DCCA and MF-DCCA methods to study the relationship between the flow fluctuations of four rivers (Daugava, Holston, Nolichucky, and French Broad) and sunspots. The results showed that there is a fractal cross-correlation between the sunspot activity time series and the river flow fluctuation time series. Shi [4] used the DCCA method to analyze the cross-correlation between the previous 15 years of rainfall, daily average temperature, PM_{10} and environmental dioxins in Hong Kong. The results indicated that when the time scale was between one month and one year, rainfall, PM_{10} and environmental dioxins exhibited long-range cross-correlation; however, when the scale was greater than one year, there was no cross-correlation between daily average temperature and environmental dioxins. Shen et al. [5] used DCCA and MF-DCCA to explore the cross-correlation at different scales between the air quality index of individual pollutants and wind speed, relative humidity, rainfall and other meteorological factors in Nanjing over a period of 12 consecutive years. The results showed persistence in the relationship between AQIs and the difference in daily temperature, and the relationship between wind speed, relative humidity and rainfall on differing scales exhibited anti-persistence.

However, correlation does not necessarily indicate causality. Inspired by Cao et al. [6], this paper introduces the use of asymmetric MF-DCCA methodology based on fluctuation conduction to study the relationship between the AQI and $PM_{2.5}$ concentration in Hangzhou. Most of the current research only considers the fractal features of the cross-correlation, whereas we explore further the fluctuation conduction of the fractal features. This paper is presented as follows: an introduction of the nonlinear Granger causality test; the introduction of the asymmetric MF-DCCA method based on fluctuation conduction; discussion of the empirical research; and, presentation of conclusions and outlook.

2. Nonlinear Granger Causality Test

In information theory, the correlation integral method is the most common method used to test causality for two time series, and is derived from a method proposed by Baek and Brock [7] to test the nonlinear causality of a series. Specially, this method can detect the correlation according to the average probability of the state similarity of two vectors. The correlation integral is as follows:

$$\begin{aligned} V_V(\varepsilon) &= P(\|V_1 - V_2\| \le \varepsilon) \\ &= \iint I_{(\|x-y\|\le\varepsilon)} f_V(x) f_V(y)\, dx dy, \end{aligned} \quad (1)$$

where V_1, V_2 *indep.*$\sim V$.

The H-J test proposed by Hiemstra and Jones [8] widened the independence hypothesis of the aforementioned method, allowing for the existence of weak correlation in the time series and thus improving the properties of small samples. Because of the normality of statistical distribution, the H-J test has become the most popular test method of nonlinear causality in economics and other fields. This paper addresses the nonlinear causality in an air pollution series. The specific method is described below.

Given two time series $\{X_t\}$ and $\{Y_t\}$, that are strictly stable and weakly dependent, then a vector and its lag vector are constructed as follows:

$$\begin{cases} X_t^m \equiv (X_t, X_{t+1}, \ldots, X_{t+m-1}), \\ Y_t^m \equiv (Y_t, Y_{t+1}, \ldots, Y_{t+m-1}), \\ X_{t-\Delta t_1}^{\Delta t_1} \equiv (X_{t-\Delta t_1}, X_{t-\Delta t_1+1}, \ldots, X_{t-1}), \\ Y_{t-\Delta t_2}^{\Delta t_2} \equiv (Y_{t-\Delta t_2}, Y_{t-\Delta t_2+1}, \ldots, Y_{t-1}), \end{cases} \quad (2)$$

where

$$\begin{cases} m = 1,2,\ldots; \quad t = 1,2,\ldots; \\ \Delta t_1 = 1,2,\ldots; \quad t = \Delta t_1 + 1, \Delta t_1 + 2, \ldots; \\ \Delta t_2 = 1,2,\ldots; \quad t = \Delta t_2 + 1, \Delta t_2 + 2, \ldots. \end{cases}$$

For a given m, Δt_1, $\Delta t_2 > 1$ and $e > 0$, the time series $\{Y_t\}$ fails the nonlinearity Granger cause $\{X_t\}$ if:

$$\begin{aligned} &\Pr\left(\left\|X_t^m - X_s^m\right\| < e \;\middle|\; \left\|X_{t-\Delta t_1}^{\Delta t_1} - X_{s-\Delta t_1}^{\Delta t_1}\right\| < e, \left\|Y_{t-\Delta t_2}^{\Delta t_2} - Y_{s-\Delta t_2}^{\Delta t_2}\right\| < e\right) \\ &= \Pr\left(\left\|X_t^m - X_s^m\right\| < e \;\middle|\; \left\|X_{t-\Delta t_1}^m - X_{s-\Delta t_1}^m\right\| < e\right), \end{aligned} \quad (3)$$

where $\Pr(\cdot)$ indicates the probability density and $\|\cdot\|$ indicates the maximum norm.

The probability is marked as follows:

$$\begin{cases} C1(m+\Delta t_1, \Delta t_2, e) \\ \quad \equiv \Pr\left(\left\|X_{t-\Delta t_1}^{m+\Delta t_1} - X_{s-\Delta t_1}^{m+\Delta t_1}\right\| < e, \left\|Y_{t-\Delta t_2}^{\Delta t_2} - Y_{s-\Delta t_2}^{\Delta t_2}\right\| < e\right), \\ C2(\Delta t_1, \Delta t_2, e) \\ \quad \equiv \Pr\left(\left\|X_{t-\Delta t_1}^{\Delta t_1} - X_{s-\Delta t_1}^{\Delta t_1}\right\| < e, \left\|Y_{t-\Delta t_2}^{\Delta t_2} - Y_{s-\Delta t_2}^{\Delta t_2}\right\| < e\right), \\ C3(m+\Delta t_1, e) \\ \quad \equiv \Pr\left(\left\|X_{t-\Delta t_1}^{m+\Delta t_1} - X_{s-\Delta t_1}^{m+\Delta t_1}\right\| < e\right), \\ C4(\Delta t_1, e) \equiv \Pr\left(\left\|X_{t-\Delta t_1}^{\Delta t_1} - X_{s-\Delta t_1}^{\Delta t_1}\right\| < e\right). \end{cases} \quad (4)$$

Then the null hypothesis of Eq. (3) is developed into a conditional probability form as follows:

$$H_0: \frac{C1(m+\Delta t_1, \Delta t_2, e)}{C2(\Delta t_1, \Delta t_2, e)} = \frac{C3(m+\Delta t_1, e)}{C4(\Delta t_1, e)}. \quad (5)$$

$I(Z_1, Z_2, e)$ indicates the indicative function, which is equal to 1 when two conformable vectors, Z_1 and Z_2, are within the maximum-norm distance e of each other and is equal to 0 otherwise:

$$I(Z_1, Z_2, e) = \begin{cases} 1, & \|Z_1 - Z_2\| \le e, \\ 0, & \|Z_1 - Z_2\| > e. \end{cases} \quad (6)$$

Then expand Eq. (4) is expanded as follows:

$$\begin{cases} C1(m+\Delta t_1,\Delta t_2,e) \\ \quad \equiv \dfrac{2}{n(n-1)}\sum\sum_{t<s} I\left(X_{t-\Delta t_1}^{m+\Delta t_1}, X_{s-\Delta t_1}^{m+\Delta t_1}, e\right) \\ \qquad \times I\left(Y_{t-\Delta t_2}^{\Delta t_2}, Y_{s-\Delta t_2}^{\Delta t_2}, e\right), \\ C2(\Delta t_1,\Delta t_2,e) \\ \quad \equiv \dfrac{2}{n(n-1)}\sum\sum_{t<s} I\left(X_{t-\Delta t_1}^{\Delta t_1}, X_{s-\Delta t_1}^{\Delta t_1}, e\right) \\ \qquad \times I\left(Y_{t-\Delta t_2}^{\Delta t_2}, Y_{s-\Delta t_2}^{\Delta t_2}, e\right), \\ C3(m+\Delta t_1,e) \\ \quad \equiv \dfrac{2}{n(n-1)}\sum\sum_{t<s} I\left(X_{t-\Delta t_1}^{m+\Delta t_1}, X_{s-\Delta t_1}^{m+\Delta t_1}, e\right), \\ C4(\Delta t_1,e) \\ \quad \equiv \dfrac{2}{n(n-1)}\sum\sum_{t<s} I\left(X_{t-\Delta t_1}^{\Delta t_1}, X_{s-\Delta t_1}^{\Delta t_1}, e\right), \end{cases} \tag{7}$$

where

$$\begin{cases} t,s = \max(\Delta t_1,\Delta t_2)+1,\ldots,T-m+1, \\ n = T-\max(\Delta t_1,\Delta t_2)-m+1. \end{cases}$$

The condition that the null hypothesis cannot be rejected is then converted in order to test whether the following formula is established as follows:

$$\sqrt{n}\left[\frac{C1(m+\Delta t_1,\Delta t_2,e)}{C2(\Delta t_1,\Delta t_2,e)} - \frac{C3(m+\Delta t_1,e)}{C4(\Delta t_1,e)}\right]^{\Delta t_1} \sim N\left(0,\sigma^2(m,\Delta t_1,\Delta t_2,e)\right). \tag{8}$$

3. Asymmetric MF-DCCA Method Based on Fluctuation Conduction

The MF-DCCA method can only analyze the fractal correlation at the same moment for two series, and does not analyze the direction in which the fractal fluctuations are conducted between the two series. Cao et al. [6] used an asymmetric MF-DCCA method based on fluctuation conduction to explore the conduction direction and delay time of fractal fluctuations between two time series.

Given two time series $\{x(t)\}$ and $\{y(t)\}$ which have the same length N, where $t = 1,2,\ldots,N$. The time series $\{y(t)\}$ is lagged by Δt hours, and then calculate the cumulative dispersion is calculated as follows:

$$\begin{cases} x(m) = \sum_{t=1}^{m}\left(x(t)-\bar{x}\right), \\ y(m) = \sum_{t=1}^{m}\left(y(t+\Delta t)-\bar{y}_{\Delta t}\right), \end{cases} \tag{9}$$

where $m = 1,2,\ldots,N-\Delta t$.

Although the series can effectively alleviate the autocorrelation effect after eliminating the trend, the autocorrelation of time series $\{y(t)\}$ is still retained. We make further improvements to attain higher rigorousness by adding a noise to the time series $\{y(t)\}$. In accordance with Cao et al. [6], the new series is then written as follows:

$$\begin{cases} x(m) = \sum_{t=1}^{m}\left(x(t)-\bar{x}\right), \\ y(m) = \sum_{t=1}^{m}\Big(y(t+\Delta t_2)-\bar{y}_{\Delta t_2} \\ \qquad +\alpha x(t+\Delta t_1)-\alpha\bar{x}_{\Delta t_1}\Big), \end{cases} \tag{10}$$

where $\Delta t_1 \geq \Delta t_2$, $m = N-\Delta t_1$, $\Delta t_1 < \Delta t_2$, $m = N-\Delta t_2$. The value of α is calculated as follows:

$$\begin{cases} \alpha = \dfrac{\sum_{t=1}^{m} y(t+\Delta t)^2}{(N-\Delta t_1)\sum_{t=1}^{m} x(t+\Delta t)^2}, \\ \qquad \Delta t_1 \geq \Delta t_2,\ m = N-\Delta t_1, \\ \alpha = \dfrac{\sum_{t=1}^{m} y(t+\Delta t)^2}{(N-\Delta t_2)\sum_{t=1}^{m} x(t+\Delta t)^2}, \\ \qquad \Delta t_1 < \Delta t_2,\ m = N-\Delta t_1. \end{cases} \tag{11}$$

Then the time series is split into $Nn = \mathrm{int}(N/n)$ segments of length N. In order to fully utilize the data, the same operation is taken after the time series is reversed. Thus, $2N$ segments are obtained.

Then splitting the time series into $Nn = \mathrm{int}(N/n)$ segments of length N. In order to fully utilize the data, the same operation is taken after the time series is reversed. Thus, $2N$ segments are obtained.

For each segments x_v and y_v, the least squares method is used to fit the corresponding local trend as follows:

$$\tilde{x}_v = a_{xv}+b_{xv}k, \quad \tilde{y}_v = a_{yv}+b_{yv}k, \quad k = 1,2,\ldots,n. \tag{12}$$

Then we get the wave function:

$$F_v(n) = \frac{1}{n}\sum_{k=1}^{n}\left|x_{v,k}-\tilde{x}_{v,k}\right|\cdot\left|y_{v,k}-\tilde{y}_{v,k}\right|. \tag{13}$$

In relation to the trend b_{xv} of the segment x_v, the q-order mean wave function under different trends is obtained as follows:

$$\begin{cases} F_q(n) = \left(\dfrac{1}{2Nn}\sum_{v=1}^{2Nn}\left[F^2(n,v)^{\frac{q}{2}}\right]\right)^{\frac{1}{q}}, \\ F_q^{+}(n) = \left(\dfrac{1}{M^{+}}\sum_{v=1}^{2Nn}\dfrac{\mathrm{sign}(b_{xv})+1}{2}\left[F_v(n)\right]^{\frac{q}{2}}\right)^{\frac{1}{q}}, \\ F_q^{-}(n) = \left(\dfrac{1}{M^{-}}\sum_{v=1}^{2Nn}\dfrac{-\left[\mathrm{sign}(b_{xv})-1\right]}{2}\left[F_v(n)\right]^{\frac{q}{2}}\right)^{\frac{1}{q}}, \end{cases} \tag{14}$$

Table 1. Basic statistics of the data.

Statistics	Mean	Max	Min
$PM_{2.5}$	45.618	243	3
PM_{10}	72.913	336	5
SO_2	10.799	51	3
NO_2	41.283	133	6
O_3	56.271	260	3
CO	0.817	2.236	0.346
Statistics	**Skewness**	**Kurtosis**	**J-B statistic**
$PM_{2.5}$	1.542	6.109	6998.208
PM_{10}	1.503	6.052	6695.69
SO_2	1.545	6.573	8143.465
NO_2	0.774	3.396	932.205
O_3	1.225	4.096	2630.54
CO	1.023	3.921	1837.197

where $M^+(M^-)$ indicates the number of segments that are rising (falling).

Finally, the power-law relationship between the q-order mean wave function and the length of segments n is obtained:

$$F_q(n) \sim n^{h(q)}; \quad F_q^+(n) \sim n^{h^+(q)};$$
$$F_q^-(n) \sim n^{h^-(q)}. \quad \dots\dots\dots\dots \quad (15)$$

If $h(q)$ is affected by q, then there is a multifractal of cross-correlation. If $h(q)$, $h^+(q)$, $h^-(q)$ are not equal, then it means that there are asymmetric features.

In order to explore fluctuation conduction, we consider the Hurst exponent $h(2)$: if $h(2) > 0.5$, long-term memory is indicated, and if $h(2) < 0.5$, there is a mean reply. Therefore, we can use $h(2)$ to monitor the similarity of fluctuations between two time series. When $\{y(t)\}$ lags, then the effect of $\{x(t)\}$ on $\{y(t)\}$ can be detected and we can check the influence of $\{x(t)\}$ on $\{y(t)\}$. Conversely, when $\{x(t)\}$ lags, then the effect of $\{y(t)\}$ on $\{x(t)\}$ can be detected.

4. Empirical Analysis

4.1. Data Sources and Description

This paper has selected Hangzhou AQI data, which includes the indices of six pollution factors ($PM_{2.5}$, PM_{10}, SO_2, NO_2, O_3, and CO). The time period chosen for hourly data is from March 1, 2016, to February 28, 2017. The length of the selected time series is 8,760 hours; the rate of missing hours is less than 1%. This paper adopts the sliding average filling process, in that each of the missing values is replaced by the average value from the fixed window. Additionally, this paper focuses on $PM_{2.5}$ and explores the fractal features of cross-correlation between $PM_{2.5}$ and other air quality indices.

It can be seen from **Table 1** that the skewness of each air quality index is greater than 0, indicating that the data is right-biased. The kurtosis values are greater than 3, indicating that they are all in peak tail. The values of the J-B statistic are far greater than the critical value at the 5% and 1% significant level, indicating that the data disobeys normal distribution.

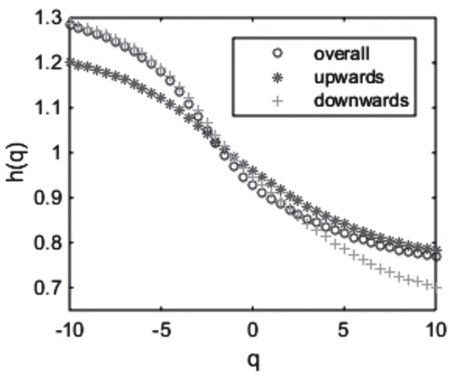

Fig. 1. Cross-correlation between $PM_{2.5}$ and PM_{10}.

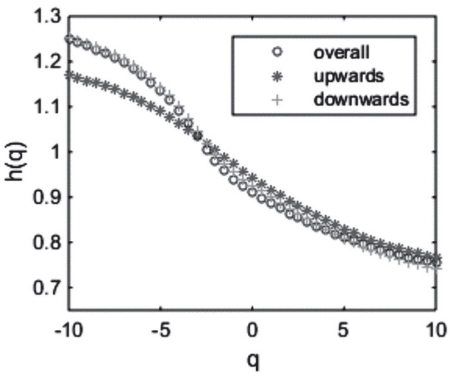

Fig. 2. Cross-correlation between $PM_{2.5}$ and SO_2.

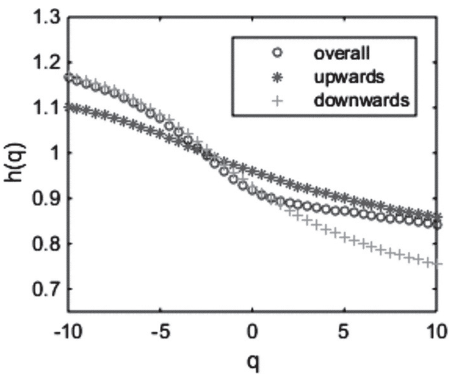

Fig. 3. Cross-correlation between $PM_{2.5}$ and NO_2.

4.2. Empirical Analysis of Asymmetric Cross-Correlation

Figures 1–5 show the asymmetric multifractal correlation between $PM_{2.5}$ and the other air quality indices in Hangzhou.

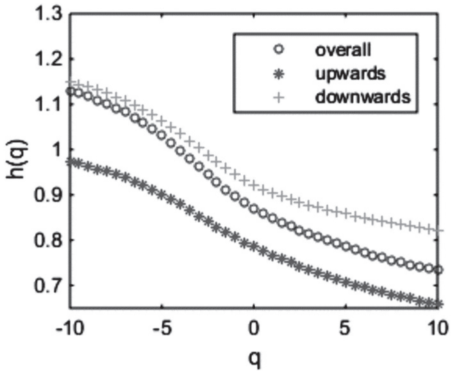

Fig. 4. Cross-correlation between $PM_{2.5}$ and O_3.

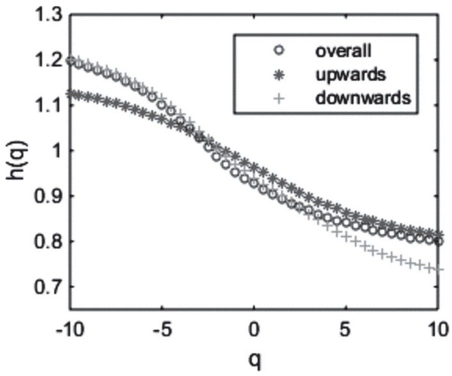

Fig. 5. Cross-correlation between $PM_{2.5}$ and CO.

Figures 1 through **5** show the generalized Hurst exponent values for the asymmetric multifractal of the cross-correlation between the AQI and $PM_{2.5}$ in Hangzhou, where q is from -10 to 10. It is obvious that the three curves in each graph do not overlap, which indicates that the cross-correlation between each AQI and $PM_{2.5}$ is asymmetric. Moreover, the curves of each graph vary with q, denoting that the cross-correlation between each AQI and $PM_{2.5}$ has multifractal features in any trend of the $PM_{2.5}$ series.

Table 2 shows the fractal characteristics of the cross-correlation between the various air quality indices and $PM_{2.5}$ in Hangzhou. It can be seen from $h(2)$ that the Hurst exponent between each AQI and $PM_{2.5}$ is greater than 0.5, indicating that there is persistence. The Hurst exponent of the overall series and the downwards trend series are close, while the Hurst exponent between each AQI (with the exception of O_3) and $PM_{2.5}$ are smaller than those of the overall series and the downwards trend series in the upwards trend, indicating that their cross-correlation persistence is weak when $PM_{2.5}$ rises, but it is stronger when $PM_{2.5}$ declines, while the other air quality indices indicate the opposite behavior. It can be seen from Δh and $\Delta\alpha$ that the fractal strength of the cross-correlation between each AQI and $PM_{2.5}$ is stronger in the overall and downward series, and weak in the upward series.

Table 2. The values of $h(2)$, Δh, $\Delta\alpha$.

	Series	$PM_{2.5}$/ PM_{10}	$PM_{2.5}$/ SO_2	$PM_{2.5}$/ NO_2	$PM_{2.5}$/ O_3	$PM_{2.5}$/ CO
$h(2)$	**Overall**	0.874	0.864	0.889	0.831	0.885
	Upwards	0.905	0.891	0.932	0.750	0.918
	Downwards	0.876	0.874	0.874	0.890	0.887
Δh	**Overall**	0.622	0.615	0.429	0.513	0.504
	Upwards	0.511	0.501	0.326	0.404	0.385
	Downwards	0.689	0.628	0.516	0.431	0.565
$\Delta\alpha$	**Overall**	1.464	1.574	1.328	1.410	1.357
	Upwards	1.213	1.235	0.993	0.948	0.903
	Downwards	1.414	1.533	1.276	1.258	1.301

Table 3. Nonlinear causality test result.

	Δt	1	2	3	4	5
$PM_{2.5}\rightarrow$ PM_{10}	**Forwards**	2.696 ***	4.211 ***	3.933 ***	3.738 ***	3.658 ***
	Backwards	4.905 ***	4.745 ***	4.59 ***	3.925 ***	3.573 ***
$PM_{2.5}\rightarrow$ SO_2	**Forwards**	1.576 *	2.142 **	1.967 **	2.004 **	1.759 **
	Backwards	2.516 ***	2.186 **	2.48 ***	2.511 ***	2.733 ***
$PM_{2.5}\rightarrow$ NO_2	**Forwards**	2.362 ***	3.509 ***	2.903 ***	2.593 ***	2.053 **
	Backwards	1.986 **	2.166 **	1.733 **	1.635 *	1.732 **
$PM_{2.5}\rightarrow$ O_3	**Forwards**	1.432 *	0.555	0.613	0.922	1.017
	Backwards	1.105	1.079	0.869	0.888	0.85
$PM_{2.5}\rightarrow$ CO	**Forwards**	2.684 ***	2.807 ***	2.507 ***	2.462 ***	2.466 ***
	Backwards	2.642 ***	2.418 ***	2.793 ***	2.332 ***	2.205 **

4.3. Nonlinear Granger Causality Test

In order to monitor the causal relationship between $PM_{2.5}$ and the various air pollutant time series, we introduced the nonlinear Granger causality test as proposed by Baek and Brock [7]. **Table 3** gives the statistical values of the mutual causality test between $PM_{2.5}$ and the other air pollution factors. We set $m = 1$, $\Delta t = Lx = Ly = 1, 2, \ldots, 5$, while ***, **, and * represent 1%, 5%, and 10% significance levels, respectively.

It can be seen from **Table 3** that the nonlinear Granger causality test statistic between $PM_{2.5}$ and four of the air pollution factors can reject the overall at a high level of significance at different orders, which demonstrates that causal relationships exist between them. It can be seen from the statistical values that the causal relationship between PM_{10} and $PM_{2.5}$ is most evident. The statistical value between O_3 and $PM_{2.5}$ can no longer reject the null hypothesis at a higher level of significance, indicating that the causal relationship between these two indices is not obvious.

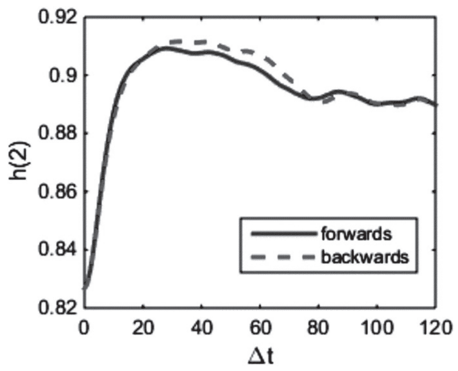

Fig. 6. Fluctuation conduction between $PM_{2.5}$ and PM_{10}.

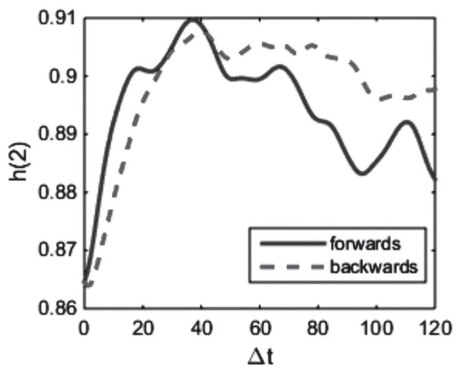

Fig. 7. Fluctuation conduction between $PM_{2.5}$ and SO_2.

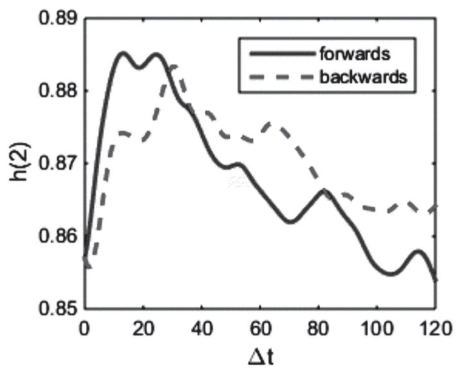

Fig. 8. Fluctuation conduction between $PM_{2.5}$ and NO_2.

4.4. Empirical Analysis of Asymmetric Fluctuation Conduction Effect

In this section, we analyze the results of the combination of fluctuation conduction with the MF-DCCA method to detect the fractal characteristics of the fluctuation conduction between $PM_{2.5}$ and the various air quality indexes. For convenience, the lag time $\Delta t_1 = \Delta t_2$, with values from 1 to 120 (for a total of 5 days).

The fluctuation conduction has been delayed, signifying that if $\{x(t)\}$ has an influence on $\{y(t)\}$, then the two series have the strongest correlation when the series $\{y(t)\}$ lags a certain order. Therefore, if $\{x(t)\}$ has a fluctuation conduction to $\{y(t)\}$, then the $h(2)$ of $\{x(t)\}$ to $\{y(t)\}$ will increase initially and then decline as Δt becomes larger and, in addition, the Δt corresponding to the maximum value of $h(2)$ is the delay time of $\{x(t)\}$ to $\{y(t)\}$. If this trend is not obvious, then $\{x(t)\}$ has no effect on $\{y(t)\}$.

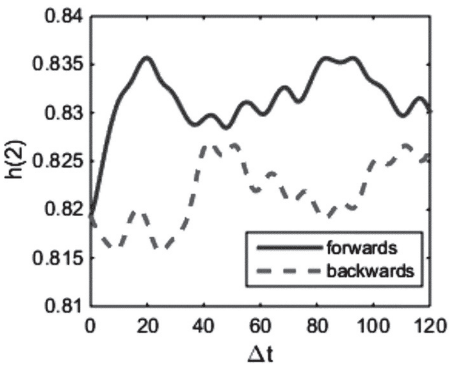

Fig. 9. Fluctuation conduction between $PM_{2.5}$ and O_3.

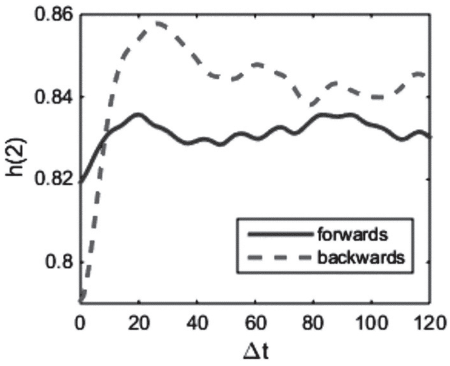

Fig. 10. Fluctuation conduction between $PM_{2.5}$ and CO.

Table 4. Fractal fluctuation conduction delay time.

	$PM_{2.5} \to PM_{10}$	$PM_{2.5} \to SO_2$	$PM_{2.5} \to NO_2$	$PM_{2.5} \to O_3$	$PM_{2.5} \to CO$
Forwards	29	38	14	21	21
Backwards	34	41	31	43	27

In **Figs. 6** through **10**, it can be seen that the fluctuation conduction between $PM_{2.5}$ and PM_{10}, SO_2, and NO_2 in Hangzhou show a significant initial increase followed by decreasing trend, indicating that there exist bidirectional fluctuation conduction between $PM_{2.5}$ and PM_{10}, SO_2, and NO_2. As shown in **Table 4**, the forward and backward fluctuation conduction delay time between $PM_{2.5}$ and PM_{10} are 29 and 34 hours, respectively. The fluctuation conduction delay time between $PM_{2.5}$ and SO_2 is about 40 hours. The forward fluctuation conduction time between $PM_{2.5}$ and NO_2 is 14 hours, while the backward fluctuation conduction takes 31 hours.

When observing the fluctuation conduction of $PM_{2.5}$ and O_3 in **Fig. 2**, it can be seen that the Hurst exponent reaches the maximum value at 21 hours in the forward conduction, but there is no significant decrease at a later point. In addition, we can see that the Hurst exponent reaches a larger value after 90 hours; therefore fluctuation conduction is not obvious. Conversely, backward conduction is less obvious. In combination with the results presented in **Table 4**, it can be concluded that there is no obvious fractal fluctuation conduction between $PM_{2.5}$ and O_3 in Hangzhou.

Finally, as indicated from the fluctuation conduction between $PM_{2.5}$ and CO, as shown in **Fig. 2**, it can be seen that both curves rise initially and then fall; however, this trend of the forward conduction curve is not obvious while, conversely, the trend of the backward conduction curve is obvious. These results show that the fractal fluctuation of $PM_{2.5}$ to CO in Hangzhou is weak, while that from CO to $PM_{2.5}$ is strong. As can be seen in **Table 4**, the fractal fluctuation conduction time of CO to $PM_{2.5}$ is 27 hours.

5. Conclusions

In our study, we determined the causal relationship between various air quality indexes and $PM_{2.5}$ in Hangzhou using the nonlinear Granger causality test. Then, using the asymmetric MF-DCCA method based on fluctuation conduction, we analyzed the value of the cross-correlation between the various air quality indexes and $PM_{2.5}$ under different delay times. The results are summarized as follows:

(1) Using the nonlinear Granger causality test, we found that there exists a bidirectional causal relationship between the four pollutants PM_{10}, SO_2, NO_2, and CO and $PM_{2.5}$ in Hangzhou; there is no obvious causal relationship between O_3 and $PM_{2.5}$.

(2) Through application of the asymmetric MF-DCCA method based on fluctuation conduction, it is observed that there is bidirectional fluctuation conduction between the three pollutants PM_{10}, SO_2, and NO_2 and $PM_{2.5}$ in Hangzhou with a delay time of fluctuation conduction of approximately one day; however, there is no obvious fluctuation conduction between O_3 and $PM_{2.5}$. In addition, there is a unidirectional fractal fluctuation conduction between CO and $PM_{2.5}$ with a conduction time of 21 hours.

Accordingly, it is necessary to consider not only the multifractal cross-correlation, but also the fluctuation conduction, when studying the fractal relationship of meteorological environmental data. The meteorological environment is a complex and chaotic system making it important to analyze the interaction between the various environmental elements. This paper provides a theoretical reference for the study of the fractal causality of an AQI. In future research, the fluctuation conduction between multiple elements will be more fully considered in order to gain a deeper understanding of the intrinsic mechanisms that influence air quality.

Acknowledgements

This work is supported by the Humanities and Social Sciences Research Project of Ministry of Education (18YJA910001), the National Statistical Science Research Project of China (2017LY51), the Zhejiang Province Key Research Project of Statistics (18TJZZ08), and the National Natural Science Foundation of China (11971432).

References:

[1] R. T. Vassoler and G. F. Zebende, "DCCA cross-correlation coefficient apply in time series of air temperature and air relative humidity," Physica A: Statistical Mechanics and its Applications, Vol.391, Issue 7, pp. 2438-2443, 2012.

[2] D. D. Kang, D. I. Lee, B.-H. Kwon, K. Kim, and J.-K. Park, "Features of the detrended cross-correlation analysis in the time series between absorbable particulate matter and meteorological factors," J. of the Korean Physical Society, Vol.63, Issue 1, pp. 10-17, 2013.

[3] S. Hajian and M. S. Movahed, "Multifractal Detrended Cross-Correlation Analysis of sunspot numbers and river flow fluctuations," Physica A: Statistical Mechanics and its Applications, Vol.389, Issue 21, pp. 4942-4957, 2010.

[4] K. Shi, "Detrended cross-correlation analysis of temperature, rainfall, PM_{10} and ambient dioxins in Hong Kong," Atmospheric Environment, Vol.97, pp. 130-135, 2014.

[5] C. Shen, C. Li, and Y. Si, "A detrended cross-correlation analysis of meteorological and API data in Nanjing. China," Physica A: Statistical Mechanics and its Applications, Vol.419, pp. 417-428, 2015.

[6] G. Cao, Y. Han, Q. Li, and W. Xu, "Asymmetric MF-DCCA method based on risk conduction and its application in the Chinese and foreign stock markets," Physica A: Statistical Mechanics and its Applications, Vol.468, pp. 119-130, 2017.

[7] E. Baek and W. Brock, "A general test for non-linear Granger causality: bivariate model," Working Paper, Iowa State University and University of Wisconsin–Madison, 1992.

[8] C. Hiemstra and J. D. Jones, "Testing for Linear and Nonlinear Granger Causality in the Stock Price-Volume Relation," The J. of Finance, Vol.49, Issue 5, pp. 1639-1664, 1994.

Name:
Chaohui Xiang

Affiliation:
School of Statistics and Mathematics, Zhejiang Gongshang University

Address:
No. 18, Xuezheng Street, Xiasha University Town, Hangzhou 310018, China

Brief Biographical History:

2016 B.S., Zhejiang Gongshang University

2016- Master's Student, School of Statistics and Mathematics, Zhejiang Gongshang University

Main Works:

- Financial risk management

Name:
Xiaozhen Hao

Affiliation:
School of Statistics and Mathematics, Zhejiang Gongshang University

Address:
No. 18, Xuezheng Street, Xiasha University Town, Hangzhou 310018, China

Brief Biographical History:
2016 M.S., Zhejiang Gongshang University
2016- Ph.D. Student, School of Statistics and Mathematics, Zhejiang Gongshang University

Main Works:
- Financial risk management

Name:
Zhenlong Chen

Affiliation:
School of Statistics and Mathematics, Zhejiang Gongshang University

Address:
No. 18, Xuezheng Street, Xiasha University Town, Hangzhou 310018, China

Brief Biographical History:
2004 D.Sc., Xidian University
2010- Deputy Dean, Professor, and Doctoral Tutor, School of Statistics and Mathematics, Zhejiang Gongshang University

Main Works:
- Stochastic processes and risk management

Name:
Wenhui Wang

Affiliation:
School of Statistics and Mathematics, Zhejiang Gongshang University

Address:
No. 18, Xuezheng Street, Xiasha University Town, Hangzhou 310018, China

Brief Biographical History:
2017 B.S., Nanyang Normal University
2017- Master's Student, School of Statistics and Mathematics, Zhejiang Gongshang University

Main Works:
- Financial risk management